

J.-P. Lanquart  
M. Kerkhofs  
E. Stanus  
J. Mendlewicz  
P. Linkowski

Sleep Laboratory, Department of  
Psychiatry, Erasme Hospital, Free  
University of Brussels, Belgium

## Sleep EEG Analysis by Linear Prediction: Frequency Changes of Slow-Wave Activity within NREM and REM Sleep Episodes in Healthy Men

### Key Words

Sleep EEG  
Spectral analysis  
Slow wave activity  
REM-NREM sleep cycle  
Linear prediction

### Abstract

The linear prediction method was applied to obtain a power spectra estimate of sleep EEG in 10 healthy young men. In order to analyze frequency changes of the slow-wave activity (EEG power in the delta band, 0.05–2.88 Hz), the delta mean frequency was computed for each 20-second sleep epoch. A mean delta mean frequency was calculated for each sleep stage in each individual. Our observations indicate that the delta mean frequency decreases during NREM periods and increases mainly at the onset of the REM episodes. This finding, in parallel with the detailed analysis of slow-wave power variations, leads to an additional description of sleep characteristics during transitions between the NREM-REM sleep episodes.

### Introduction

Spectral analysis is a common tool for analyzing human sleep EEG [1–6]. Various mathematical techniques have been applied to estimate power spectra. Typically, this estimate is carried out with either period amplitude analysis (PAA) or with the periodogram, where fast fourier transformation (FFT) is applied to the data. Comparisons between these two methods have been reported previously [7–10]. The results of these comparisons may be summarized as follows: PAA is known to separate wave incidence and amplitude accurately [11], although problems have been reported with the determination of signal frequency [12]. PAA is unable to discriminate superimposed waves, a common situation in EEG analysis. This drawback can be offset with the use of additional data filtering, but this may introduce spectral deformation [13]. Assuming signal stationarity, the periodogram can dis-

criminate superimposed waves, but cannot measure both wave amplitude and incidence [11]. This limitation may be overcome by shortening the epoch length of analysis, which also reduces the nonstationarity problem [12].

Linear prediction (LP) is a spectral analysis method commonly used in speech studies [14]. This technique is closely related to the autoregressive method, originally developed in economic time series forecasting, and to the maximum entropy method developed for geophysical data processing [15]. LP has been reported to have similar drawbacks to FFT [14]. LP spectral estimates, however, give a smoother spectrum than the periodogram which leads to a better frequency resolution, i.e., the ability to separate the spectral response of two sinusoidal components closely spaced in frequency [16]. These documented properties, discussed below, are essential for the correct identification of sleep activity in the different frequency bands.

It has been proposed previously that LP could be used for EEG analysis [17, 18]. To our knowledge, however, this method has not yet received further attention. In our laboratory, LP is used in automatic sleep analysis to detect short EEG events such as spindles, delta waves, and K-complexes [19]. The aim of the present investigation was to analyze frequency changes within the delta band of sleep in male subjects. The LP method was applied to obtain power spectra on 20-second epochs of sleep, along with a detailed analysis of the delta frequency band.

## Methods

### Subjects

The study group consisted of 10 normal male subjects aged 17–26 years (mean  $\pm$  SD:  $21.5 \pm 2.6$ ). All subjects were in excellent health and had regular sleep and wake schedules. They did not report any antecedents of mental or sleep disorders and were drug-free.

Nocturnal polysomnography was performed for each subject following an adaptation night at the Sleep Laboratory, Department of Psychiatry, Erasme Hospital, Université Libre de Bruxelles. Two electrooculograms, three electroencephalograms (EEG) and one submental electromyogram were used. The recorded EEG derivations were Fz/A1(A2), Cz/A1(A2), Oz/A1(A2), where A1 and A2 were the mastoid references. The signals were filtered through a low-pass antialiasing analog filter, with a cutoff frequency of 25 Hz. The signals were sampled at 50 Hz by a 12-bit A/D converter connected via direct memory access (LPA 11K) to a VAX-750 computer (Digital Equipment Corporation). To remove low-frequency drift and offsets, a high-pass digital filter with a cutoff frequency of 0.5 Hz was applied before further digital processing. The numerical raw data were saved on tapes. Calibration was done with a 50- $\mu$ V, 10-Hz sine wave signal. The power of the spectrum was scaled so that the power of a 50- $\mu$ V digitized sine wave was 1,250  $\mu$ V<sup>2</sup>.

Subsequent analyses, such as stage determination and spectrum computation were carried out on the sampled data, avoiding synchronization problems between the stages and the spectrum. Each 20-second epoch was visually scored according to the standard criteria [20] using a visualization program running on personal computers and operating directly on the sampled data. Epochs with artifacts were removed from the statistical analysis, on the basis of visual inspection of the polygraphic recordings.

### Linear Prediction

A complete description of LP theory is beyond the scope of this paper and may be found elsewhere [14, 15]; only essential points are discussed below. The LP model may be summarized as follows: the current value of the process is expressed as the weighted sum of immediately preceding samples, plus an error term (the prediction error). The weighting factors are the autoregression coefficients. The number of coefficients specifies the order of the prediction. The power spectrum can be derived by the application of the FFT to the autoregression coefficients, the FFT being used here as a mathematical tool.

Given  $p$  past values of a process  $x_{n-k}$  ( $k = 1, \dots, p$ ), the present sample  $x_n$  is estimated by the following linear combination

$$\hat{x}_n = -(a_1 x_{n-1} + a_2 x_{n-2} + \dots + a_p x_{n-p}), \quad (1)$$

where  $\hat{\phantom{x}}$  indicates an estimated value.

The prediction error is given by  $e_n = x_n - \hat{x}_n$ .

The unknown coefficients  $a_i$  are obtained by a least-square minimization. Through application of the autocorrelation method, the sum of the squared errors is computed over the data sequence; the minimization of this sum gives a set of equations containing the unknown coefficients. The resulting linear system has a form that ensures the stability of the model and enables computationally efficient recursive algorithms [21]. The Leroux-Guegen algorithm was chosen for its good numerical properties such as stability and precision [14]. Since the EEG signal is known only over finite interval, the use of a window becomes necessary. The windowing procedure results in leakage [22], that is, the spreading of the power into adjacent frequency regions (sidelobes).

The knowledge of the prediction coefficients  $a_k$  leads to the signal spectrum  $P_{LP}(f)$

$$P_{LP}(f) = \frac{\sigma^2 \Delta t}{\left| 1 + \sum_{k=1}^p a_k \exp(-j2\pi k \Delta t) \right|^2} \quad (2)$$

where  $\sigma^2$  is the minimized mean square prediction error [16]. The denominator of the equation may be estimated by applying the FFT to the set of values  $[1, a_1, a_2, \dots, a_p]$ . In practice, FFT is carried out for a number  $N_{FFT}$  of points equal to a power of 2 (usually 256, 512 or 1,024) [23]. If the number of coefficients for the FFT ( $p+1$ ) is less than the number of points ( $N_{FFT}$ ), zero padding is applied: the missing values ( $N_{FFT}-p-1$  values) are set to zero. It should be noted that an increase of  $N_{FFT}$  does not improve the frequency resolution, but only serves to interpolate additional values in the spectrum and therefore to resolve ambiguities [16].

There is evidence that the power spectrum (Eq. 2) of order  $p$  describes the signal with, at most,  $\text{trunc}(p/2)$  resonances, manifested in main frequency bell-shaped peaks [24]. This property ensures that the LP spectrum will not contain undesirable fluctuations. Moreover, as shown previously [16, 24], the formulation itself of the power spectrum is responsible for the high resolution property of LP spectra. Therefore, LP spectra would not be expected to exhibit sidelobes due to windowing. However, the autocorrelation method requires data windowing, thus the enhanced resolution typical of LP spectra will, in fact, be reduced by leakage.

The order  $p$  of the model must be determined before any computation can be undertaken, yet the order is generally not known a priori. An order that is too low will result in a highly smoothed spectrum, while an order that is too high will produce spurious peaks in the spectrum. Different procedures have been developed for the determination of the optimal order [16]. The order determination is essential, but not critical, since a somewhat greater value than the true values does not greatly distort the spectrum [25, 26].

### Data Analysis

LP power spectrum estimate may be completed once the spectrum order  $p$  is defined. As discussed above, the order is a function of the signal and the objective of the study. For a spectrum estimate on a 20-second window, numerical tests give as optimal order  $p = 18$ . FFT is then applied to the 18 autoregression coefficients to obtain the power spectra. Since FFT is computed with a number of  $N_{FFT}$  of points equal to 1,024, zero padding is applied, as explained in the LP section above.

We analyzed the frequency variations within the delta band in nocturnal polysomnographic recordings obtained from 10 normal male subjects. LP power spectrum was computed on each 20-second epoch of sleep for the central EEG derivation. We present results obtained on the full spectrum within the delta band. Each delta spectrum may be seen as the statistical distribution of power (observed character) as a function of frequency (independent variable). Descriptive information, such as the mean, can then be computed by the classical formula of descriptive statistics [27]. The limits for the delta band were fixed between 0.05 and 2.88 Hz. This frequency range was selected because it always includes the delta peak, without any extension over the other frequency bands. This ensures that the descriptive information for the delta peak are not perturbed by the adjacent power peak in the spectrum.

The statistical procedure used in this study was the one-way analysis of variance with repeated measures [28].

## Results

The study was initiated by the inspection of the individual spectra of all subjects. Figures 1 and 2 show a detailed spectrum (0–5 Hz) of one stage 2 and one stage 3 epoch for a representative subject. As expected, delta power is much higher in stage 3 than in stage 2. It can also be seen that the position of the delta peak (0.05–2.88 Hz) changes on the frequency axis across the two stages. To analyze in detail these frequency changes, individual spectra were computed for each 20-second epoch of sleep in all 10 subjects. The delta frequency changes are described by the mean frequency, computed for each 20-second epoch. This variable is referred to as the DMF (delta mean frequency). Figure 3 illustrates the hypnogram and the power in the delta band together with the temporal evolution of the DMF for a representative subject. In the two middle panels of this figure, each value has been replaced by a moving average on 11 consecutive epochs (3 min 40 s) to reduce epoch variability. To analyze the stage effect, the DMF values were grouped per stage for each subject. This procedure gives a complete set of DMF values for each stage. The mean and standard deviation were computed for each set of DMF for each subject.

Table 1 gives the mean DMF values and the statistical weight for each stage in all 10 individuals. Identical statistical weight implies identical epoch number for each stage. To take into account the variable number of epochs for each stage, a stage weight is introduced in the computation of the statistical procedure for each stage of each subject. The definition of this weight is similar to that used in the field of the weighted least-squared approximation. For each subject, the weight of a stage is proportional to the number of epochs for the stage considered. The proportionality factor of the statistical weights is defined so

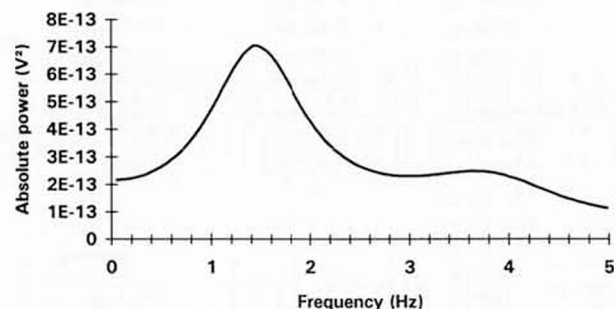


Fig. 1. LP spectrum of one stage 2 epoch.

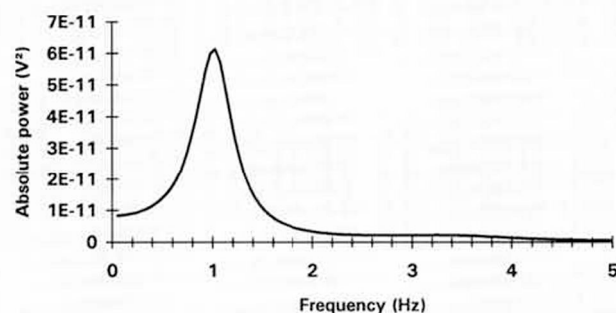
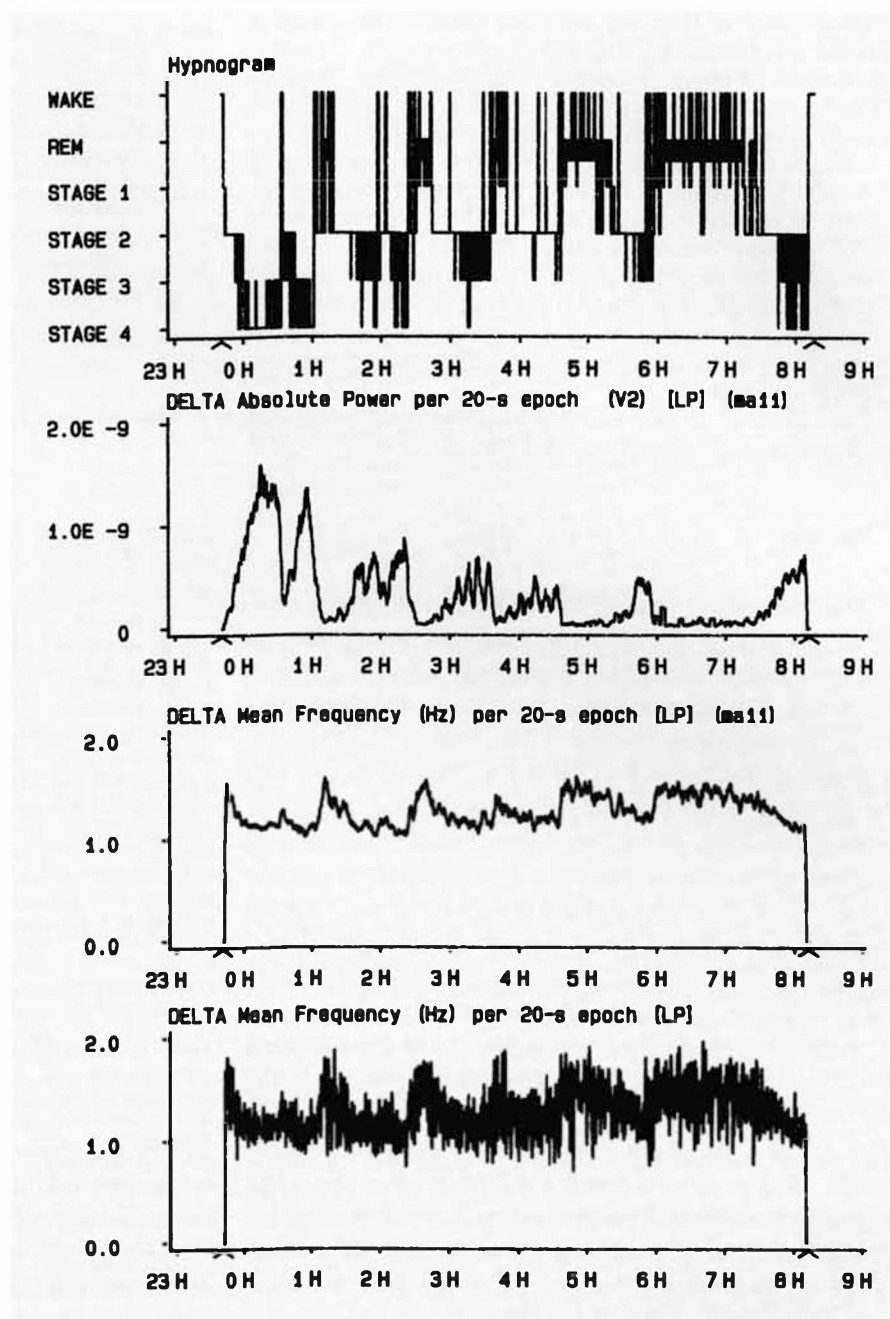


Fig. 2. LP spectrum of one stage 3 epoch.

that the sum of the 6 weights for 1 subject remains equal to the number of variables, in this case the 6 stages. This normalization procedure ensures that each subject has an identical statistical weight (total statistical weight of one subject = 6). This table also shows the global mean DMF for each stage calculated for the group of 10 subjects, and the total weight of each stage. It is important to note that all values in table 1 were computed without any preliminary averaging of the DMF on consecutive epochs, as this operation would result in a mixing of stage values.

The value of the Fisher statistic [28] for the analysis of variance with repeated measures of the DMF values in table 1 was  $F_{5,45} = 92.17$  ( $p < 0.01$ ). Sleep stages presented in table 1 can be ordered according to increasing global mean DMF values: stage 3, stage 4, wake, stage 2, stage 1, REM stage. In order to obtain additional information on the significant differences between stages, a posteriori tests were performed according to the Newman-Keuls procedure [28]. Applied to the global mean DMF values of the sleep stages, this test divides the set of ordered



**Fig. 3.** Hypnogram (upper panel) and temporal evolution of delta power (middle panel) and delta mean frequency (two lower panels) for a representative subject. ma11: Moving average = 11 epochs.

means into subsets that are consistent with the hypothesis of no differences. Table 2 presents the differences of global mean DMFs between two sleep stages. When an observed difference between two sleep stages exceeds the Scheffé critical value ( $c = 0.073$  for  $p = 0.01$ ,  $c = 0.087$  for  $p = 0.001$ ), the hypothesis of equality between two corresponding sleep stages is rejected at the 0.01 or 0.001 level of significance. These results demonstrate that the upper mean DMF value of the REM stage is statistically differ-

ent from values of other stages. Moreover, the lower mean DMF values for stages 3 and 4 cannot be statistically differentiated, while they are statistically different from other sleep stages (see tables 1, 2).

The variation of the DMF values during the transition from the NREM to REM episodes were then analyzed among the 47 NREM-REM transitions available in the sample. When REM sleep was preceded by sleep stage shifts between wake, stage 1, or stage 2, two modes of tran-

**Table 1.** Individual mean delta mean frequencies and statistical weights for each sleep stage

No.	Wake	Stage 1	Stage 2	Stage 3	Stage 4	REM
1	1.175 0.49	1.368 0.34	1.209 3.04	1.089 0.55	1.062 0.13	1.498 1.45
2	1.273 1.12	1.419 0.41	1.376 1.94	1.205 0.33	1.228 0.79	1.454 1.41
3	1.211 0.64	1.410 0.21	1.346 3.60	1.271 0.30	1.323 0.03	1.534 1.21
4	1.120 0.32	1.416 0.28	1.251 2.82	1.090 0.67	1.095 0.56	1.507 1.35
5	1.376 0.64	1.499 0.32	1.369 31.7	1.238 0.35	1.217 0.26	1.543 1.27
6	1.260 0.56	1.435 0.56	1.343 3.25	1.137 0.39	1.099 0.48	1.509 0.75
7	1.212 0.37	1.406 0.25	1.231 2.28	1.065 0.63	1.075 0.88	1.430 1.59
8	1.252 0.75	1.424 0.23	1.326 2.92	1.222 0.24	1.270 0.82	1.464 1.04
9	1.247 0.27	1.488 0.17	1.311 3.11	1.178 0.55	1.196 0.71	1.551 1.18
10	1.263 0.60	1.376 0.19	1.429 3.08	1.246 0.35	1.249 0.54	1.584 1.24
Global mean	1.250	1.425	1.321	1.155	1.176	1.505
Total weight	5.76	2.97	29.22	4.35	5.21	12.49

sition were detected. In 22 NREM-REM transitions, the DMF increase started gradually during these stage shifts and reached a maximum when REM occurred. This gradual DMF increase was present in up to 50 consecutive 20-second sleep epochs preceding the REM stage. Another mode of DMF increase was detected in 4 transitions: the increase took place abruptly, on less than three consecutive 20-second sleep epochs. In 21 NREM-REM transitions where no stage shift between wake, stage 1 or 2 was present before the REM stage, a sharp DMF increase was observed when the REM stage occurred. It should be pointed out that 4 subjects out of 10, with a total of 18 NREM-REM transitions, exhibited 17 gradual DMF increases, suggesting that this mode of DMF increase could be specific to some subjects.

DMF increases were also analyzed in the reverse order: the gradual and rapid DMF increases were identified on curves of DMF values plotted as a function of time. Here, the mean and the standard deviation were

**Table 2.** Multiple comparisons between mean DMF values of sleep stages: differences between the mean DMF values

	Stage 3	Stage 4	Wake	Stage 2	Stage 1	REM
Stage 3		0.022	0.096**	0.166**	0.270**	0.350**
Stage 4			0.074*	0.145**	0.248**	0.329**
Wake				0.070	0.174**	0.254**
Stage 2					0.104**	0.184**
Stage 1						0.080*

Sleep stages ordered according to increasing mean DMF values, see table 1.

\*  $p < 0.01$ ; \*\*  $p < 0.001$ .

computed on windows of 10 consecutive 20-second sleep epochs of the DMF curve. Let us consider a 10-epoch window, which we will refer to as the current window. Since a gradual increase leads to a long-term trend in the DMF values, such an increase was detected by comparison of the mean values of consecutive 10-epoch windows. A gradual DMF increase was identified when the means, computed on 3 consecutive 10-epoch windows (the current one and the next two windows), increased successively more than one-half of the standard deviation of the current window.

A rapid DMF increase leads to a sudden change in the DMF values of the 20-second epochs, followed by a higher mean on the next 10-epoch window than the current mean. A rapid DMF increase was suspected when consecutive DMF values, on at least three 20-second sleep epochs, were 2 standard deviations greater than the mean value of the current 10-epoch window. A rapid increase was then identified when the mean value of the following 10-epoch window was also 2 standard deviations greater than the current 10-epoch window. If no DMF increase was detected, the current window was replaced by the following window, and the search started again. This simple approach allows for a comparison between DMF increases and REMP occurrences. Fifty DMF increases were observed: the 47 already detected with a NREM-REM transition and 3 additional DMF increases that were not associated with sleep transition. Among these 3 DMF increases, 2 occurred during the first NREM period for 2 subjects with REM latencies of 143 and 156 min, respectively. The third of these DMF increases occurred during sleep stage shifts between wake, stages 1 and 2, followed by a short-duration DMF decrease, and then followed by a rapid DMF increase corresponding finally to the occurrence of REM.



## Discussion

Our data indicate that the delta mean frequency (referred to as the DMF) is dependent on sleep stage. We also demonstrate that DMF decreases during NREM periods (NREMP), and increases mainly at the onset of REM episodes. Furthermore, we find that a DMF increase occurs consistently during each of the 47 NREM-REM transitions available in our sample, while only 3 significant DMF increases are not linked to sleep stage transitions.

It has already been noted that delta frequency, defined as frequency at which the maximum power is located, decreases as stage 4 progresses during the night, from NREMP 1 to NREMP 3 [29]. We report here a different and more complex evolution of the DMF that appears to be a function of the NREM-REM sleep cycles. Our results indicate that DMF decreases during NREMP while it increases during REM. It should be pointed out that these frequency oscillations occur even when delta power is reduced, as in the last sleep cycles. Our results are also consistent with a recent contribution [30] where the delta frequency range is divided into 4 ranges (0.5–0.75, 0.75–1.0, 1.0–1.5 and 1.5–2.0 Hz). These authors show that the slower frequency bands are increased during the first NREMP. However, the frequency resolution in that analysis appears to be insufficient to clearly identify the frequency changes within the delta range.

As noted by Feinberg et al. [31], NREMP duration is typically determined by visual assessment. Thus, the scorer must determine visually that REM has appeared, this marking the end of the NREM period. Our results demonstrate that REM occurs with a significant increase of the DMF, always preceded by a delta power decrease. We propose that this new information be taken into account to determine NREMP end. Through simultaneous inspection of the hypnogram, delta power and DMF, NREM period would be limited by REM stage occurrence correlated with a DMF increase. This approach adds two intrinsic properties of SWS – delta power and DMF changes – to NREM period determination, and is not exclusively based on visual scoring. We observed both gradual and rapid significant DMF increases at each NREM-REM transition. It seems that some subjects may present only gradual DMF increases. However, a larger number of subjects are required to analyze in detail whether the mode of DMF increase could identify particular subgroups.

Our results also show that a REM stage occurs with a DMF increase while the opposite is not necessarily true. In the 47 available NREM-REM transitions, a DMF

increase was systematically detected. Three more DMF increases were observed but these were not related to REM stage transition.

It should be noted that the definition of a significant event on a curve is dependent on the objective of the study. The numerical values for the definition of a significant DMF increase – window length, number of consecutive values, increase threshold – were fixed to detect the minimum number of increases, including the 47 increases during NREM-REM transitions. A gradual DMF increase was detected using a 10-epoch window, which lasts 3.33 min, while a rapid DMF increase was detected using the 20-second sleep epochs. Since it is not our objective to detect all DMF increases, the time resolution of the 10-epoch window is not too large for the detection of the significant gradual increase. In light of this, it seems that a very small number of DMF increases (3 out of 50) are not linked to any sleep stage transition. Interestingly, a significant DMF increase without sleep transition was detected during the first NREM period of 2 subjects with a long REM latency (143 and 156 min). This finding points to work by Feinberg and March [32], indicating the difficulty of accurate REM detection when the NREM period includes two or more delta peaks. Further analyses on more subjects presenting a long REM latency are needed to clarify the problem of the so-called 'skipped' REM episodes.

We realize that our approach may not be fully satisfactory because it does not allow for any statistic. The average time course of transition for the DMF values and the delta energy could have been computed. However, the shape of variations of these variables from one NREMP to another is highly variable, both within and across subjects. This variability has already been noted for delta energy [33]. Moreover, some NREM-REM sleep transitions are gradual, while others are rapid. Therefore, the average time course of transition gives a value that does not represent individual variations. We have concentrated our study on the NREM-REM transitions because we did not detect a relationship between the variations of the DMF values and the REM-NREM transitions in all cases. Subsequent analyses are required to clarify some questions raised by these results: what is a significant DMF increase or decrease? Are they related to some changes in sleep? Why are some REM-NREM transitions free from DMF variations? Despite these questions, our results present useful and novel suggestions. We hope that other researchers will be motivated to further verify, complete, and develop these results.

Our results have been obtained with a nonconventional delta frequency range. Different values for the limits of

the delta band may be found in the literature. Aeschbach and Borbély [6] used a range of 0.25–4 Hz, while Armitage and Roffwag [4] defined the band at 0.5 to <4 Hz. Using a high-pass filter with a cutoff frequency of 0.3 Hz, Feinberg et al. [31] worked with a range of 0–3 Hz. In another study, Kuwahara et al. [34] limited delta-1 at 0.5–2 Hz and delta-2 at 2–4 Hz. A range of 0.23–2.5 Hz was employed by Mendelsohn et al. [35], and one of 0.3–3 Hz by Uchida et al. [5]. In Brunner et al. [36], the SWA is limited between 0.75 and 4.5 Hz. Such varied and divergent ranges employed by others in the field indicate that the boundaries of the delta frequency band have not yet been fully resolved.

We propose here to define the delta band from 0.05 to 2.88 Hz. The lower limit is given by the first frequency value of the spectral analysis. It extends beyond the cutoff frequency of the high-pass filter to include the whole delta resonance, as discussed in the Methods section. The superior value can be justified by inspection of figures 1 and 2. These figures present two power peaks in the range of 0–5 Hz. It should be noted that each spectral method has specific properties that lead to a specific model for the spectrum. The LP model results in a spectrum including some resonances, or bell-shaped peaks, avoiding undesirable fluctuations. These resonances explain the presence of power in the delta band below 0.5 Hz (fig. 1, 2), despite high-pass filtering with a cutoff at 0.5 Hz of the recorded data. The extra power is a consequence of resonance modelling affecting the total delta power. It should be noted that this high-pass filtering removes some true EEG power that is present below the cutoff frequency. Further analyses with different cutoff frequencies are required to correctly assess the filter effect. The first resonance (0.05–2.88 Hz) has been selected for this study. We carefully verified each of the ten polysomnographies to ensure that these limits always include the first and only the first resonance. It is obvious that the DMF value is dependent on the selected upper frequency limit. The delta band has been limited at 2.88 Hz since higher frequencies correspond to another power peak that may not present similar time variations to the first resonance. These limits ensure that the statistical descriptive information, such as the mean, are relative only to the first resonance, without any perturbation from the adjacent power peak.

Our results have been obtained using the mean frequency of the power in the delta band (0.05–2.88 Hz). Other variables could have been selected such as median frequency, mode, or peak power frequency. The peak power frequency was not selected because a single spectrum value is too sensitive to small fluctuations, due to the

noise in the spectrum. Calculations with the median frequency led to nearly identical results (Fisher statistic for analysis of variance  $F_{5,45} = 86.74$ ). The mean was preferred, however, because it averages the noise in the spectrum, while the median does not, since it is itself a single value of the spectrum. Even though the mean is rather sensitive to the extreme values, this did not influence our analysis because of the nearly symmetrical power peaks in the spectrum [27].

Our results have been obtained with a spectral analysis based on LP. The true spectrum of a signal is known only if the exact model of the signal is known. If this is not the case, the data are to be described by an acceptable model, that enables the computation of the power spectrum. It has been shown that the LP model could adequately represent the EEG [37] since the brain electrical activity is assumed to be, to a certain degree, generated by a stochastic process [38]. Further studies are needed to compare results obtained by LP, the periodogram (FFT applied directly to the data) and also with the recently developed nonlinear EEG analysis [39, 40].

In conclusion, our results indicate that DMF oscillations between SWS and REM, correlated with delta power peaks, consistently enable NREMP end determination. These intrinsic properties of SWS make it possible to characterize the NREMP physiological limits more accurately. However, it is obvious that further studies with other frequency ranges are essential to more objectively estimate sleep cycle limits.

Our observations add some additional questions. These DMF oscillations have been observed in healthy young men with normal sleep. Further studies are needed to test our modified method of NREMP determination and to check whether it may be applied to women, older normal subjects, or subjects presenting two delta power peaks in the first NREMP. Furthermore, application of this method to patients with sleep or psychopathological illnesses may also show whether this new analytical approach may improve diagnostic classification and our understanding of the physiology of sleep disorders.

## Acknowledgements

We thank C. Kempnaers, B. Jacques, B.D. Detroux, F. Lucas, D. Wasnaire, M. Coppens and N. Haverals for their technical assistance. We thank Sarah Rivelli for her comments on the manuscript.

This work was supported by a grant from the Belgium Fonds de la Recherche Scientifique Médicale, the Association pour l'Etude de la Santé Mentale, and the Hôpital Erasme.

## References

- 1 Feinberg I, Floyd TC, March JD: Effects of sleep loss on delta (0.3–3 Hz) EEG and eye movement density: New observations and hypotheses. *Electroencephalogr Clin Neurophysiol* 1987;67:217–221.
- 2 Dijk DJ, Beersma DGM: Effects of SWS deprivation on subsequent EEG power density and spontaneous sleep duration. *Electroencephalogr Clin Neurophysiol* 1989;72:312–320.
- 3 Kupfer DJ, Frank E, Ehlers CL: EEG sleep in young depressives: First and second night effects. *Biol Psychiatry* 1989;25:87–97.
- 4 Armitage R, Roffwarg HP: Distribution of period-analysed delta activity during sleep. *Sleep* 1992;15:556–561.
- 5 Uchida S, Maloney T, Feinberg I: Beta (20–28 Hz) and delta (0.3–3 Hz) EEGs oscillate reciprocally across NREM and REM sleep. *Sleep* 1992;15:352–358.
- 6 Aeschbach D, Borbély AA: All-night dynamics of the human sleep EEG. *J Sleep Res* 1993;2:70–81.
- 7 Geering B, Eggimann F, Borbély AA: EEG changes during sleep analysed by period-amplitude analysis and spectral analysis. *J Sleep Res* 1992;1(suppl 1):80.
- 8 Geering B, Eggimann F, Borbély AA: Period-amplitude analysis of the sleep EEG: Methodological considerations. *J Sleep Res* 1992;1(suppl 1):80.
- 9 Armitage R, Fitch T, Hoffman R: Comparison of period and spectral analysis in quantifying sleep EEG in depression. *J Sleep Res* 1994;3(suppl 1):9.
- 10 Armitage R, Hoffman R, Fitch T: Comparison of period and spectral analysis in quantifying sleep EEG in normal controls. *J Sleep Res* 1994;3(suppl 1):9.
- 11 Ktonas PY, Gosalia AP: Spectral analysis vs. period-amplitude analysis of narrowband EEG activity: A comparison based on the sleep delta-frequency band. *Sleep* 1981;4:193–206.
- 12 Geering BA, Achermann P, Eggimann F, Borbély AA: Period-amplitude analysis and power spectral analysis: A comparison based on all-night sleep EEG recordings. *J Sleep Res* 1993;2:121–129.
- 13 Ktonas PY: Editorial comment: Period-amplitude EEG analysis. *Sleep* 1987;10:505–507.
- 14 Boite R, Kunt M: *Traitement de la parole*. Lausanne, Presses Polytechniques Romandes, 1987.
- 15 Wei WWS: *Time Series Analysis*. London, Addison-Wesley, 1990.
- 16 Kay SM, Marple SL Jr: Spectrum analysis – a modern perspective. *Proc IEEE* 1981;69:1380–1419.
- 17 Burch NR: Automatic analysis of EEG: A review and classification of systems. *Electroencephalogr Clin Neurophysiol* 1959;11:827–834.
- 18 Barlow JS: Computerized clinical electroencephalography in perspective. *IEEE Trans Biomed Eng* 1979;26:377–391.
- 19 Stanus E, Lacroix B, Kerkhofs M, Mendlewicz J: Automated sleep scoring: A comparative reliability study of two algorithms. *Electroencephalogr Clin Neurophysiol* 1987;66:448–456.
- 20 Rechtschaffen A, Kales A: *A Manual of Standardized Terminology, Techniques and Scoring System for Sleep Stages of Human Subjects*. Los Angeles, Brain Information Service/Brain Research Institute, University of California, 1968.
- 21 Makhoul J: Linear prediction: A tutorial review. *Proc IEEE* 1975;63:561–580.
- 22 Oppenheim AV, Schaffer RW: *Digital Signal Processing*. Englewood Cliffs, Prentice-Hall, 1975.
- 23 Oppenheim AV, Willsky AS, Young IT: *Signals and Systems*. Englewood Cliffs, Prentice-Hall, 1983.
- 24 Schroeder MR: Linear prediction, external entropy and prior information in speech signal analysis and synthesis. *Speech Commun* 1982;1:9–20.
- 25 Madhavan PG, Stephens BE, Klingberg D, Morzorati S: Analysis of rat EEG using autoregressive power spectra. *J Neurosci Methods* 1991;40:91–100.
- 26 Gersch W: Spectral analysis of EEG's by autoregressive decomposition of time series. *Math Biosci* 1970;7:205–222.
- 27 Sachs L: *Applied Statistics, a Handbook of Techniques*, ed 2. New York, Springer, 1994.
- 28 Winer BJ: *Statistical Principles in Experimental Design*, ed 2. New York, McGraw-Hill, 1971.
- 29 Church MW, March JD, Hibi S, Benson K, Cavness C, Feinberg I: Changes in frequency and amplitude of delta activity during sleep. *Electroencephalogr Clin Neurophysiol* 1975;39:1–7.
- 30 Hamada M, Tagaya H, Yamamoto R, Shiotsuka S, Takahashi K, Atsumi Y, Toru M: Power densities of delta waves in sleep EEG. *J Sleep Res* 1994;3(suppl 1):97.
- 31 Feinberg I, Floyd TC, March JD: Acute deprivation of the terminal 3.5 hours of sleep does not increase delta (0–3-Hz) electroencephalograms in recovery sleep. *Sleep* 1991;14:316–319.
- 32 Feinberg I, March JD: Cyclic delta peaks during sleep: Result of a pulsatile endocrine process? *Arch Gen Psychiatry* 1988;45:1141–1142.
- 33 Armitage R, Hoffman R, Moffitt A, Pechacek P, Kiger B, Roffwarg HP: Trends in delta EEG across NREMPs: A comparison of wave amplitude and incidence. *J Sleep Res* 1992;1(suppl 1):13.
- 34 Kuwahara H, Higashi Y, Mizuki Y, Matsunari S, Tanaka M, Inanaga K: Automatic real-time analysis of human sleep stages by an interval histogram method. *Electroencephalogr Clin Neurophysiol* 1988;70:200–229.
- 35 Mendelson WB, Sack DA, James SP, Martin JV, Wagner R, Garnett D, Milton J, Wehr TA: Frequency analysis of sleep EEG in depression. *Psychiatry Res* 1987;21:89–94.
- 36 Brunner DP, Dijk D-J, Borbély AA: Repeated partial sleep deprivation progressively changes the EEG during sleep and wakefulness. *Sleep* 1993;16:100–113.
- 37 Fenwick P, Michie P, Dollimore J, Fenton G: Mathematical simulation of the electroencephalogram using an autoregressive series. *Biomed Comput* 1971;2:281–307.
- 38 Rösche J, Fell J, Beckmann P: The calculation of the first positive Lyapunov exponent in sleep EEG data. *Electroencephalogr Clin Neurophysiol* 1993;86:348–352.
- 39 Fell J, Rösche J, Beckmann P: Deterministic chaos and the first positive Lyapunov exponent: A nonlinear analysis of the human electroencephalogram during sleep. *Biol Cybern* 1993;69:139–146.
- 40 Achermann P, Hartmann R, Gunzinger A, Guggenbühl W, Borbély AA: All-night sleep EEG and artificial stochastic control signals have similar correlation dimensions. *Electroencephalogr Clin Neurophysiol* 1994;90:384–387.